hydrophobic and have a relatively large width. If one reduces the hydrophobicity or the width of such a stripe, the bridge formation will nucleate a spreading process that leads to the complete coverage of the hydrophobic stripe and to the coalescence of the channels.

Wettability patterns where pairs (or multiplets) of hydrophilic stripes have a smaller hydrophobic separation could be used as fluid microchips or microreactors. First, the different channels on the stripe pairs (or multiplets) would be filled with different reactants. Secondly, the coalescence of these channels could be induced by simply increasing their volume. In this way, small amounts of reactants could be prepared in a well-mixed state without any stirring.

Stable bridges may be placed at controlled positions by using striped surface domains with a nonuniform width or with corners (Fig. 5). In this way, one may create 2D networks of microchannels. When filled with electrolytes, one obtains another type of microchip, because the channels now act as ionic conductors.

Finally, after a certain pattern of liquid channels and bridges has been created, one may want to stabilize it by freezing, polymerization, or sol-gel reactions. When the volume change at such a phase transformation is small, the shape of the liquid pattern will be conserved. In this way, one should be able to produce both rigid and soft structures with a large variety of morphologies between two and three dimensions (*15*).

References and Notes

1. G. P. Lopez, H. A. Biebuyck, C. D. Frisbie, G. M. Whitesides, *Science* **260**, 647 (1993); J. Drelich, J. D. Miller, A. Kumar, G. M. Whitesides, *Colloids Surf. A* **93**, 1 (1994).
2. F. Morhard *et al.*, *Electrochem. Soc. Proc.* **97**, 1058 (1997).
3. K. Jacobs *et al.*, in *Proceedings of the 2nd European Coating Symposium, Strasbourg, 1997*, in press.
4. R. Wang *et al.*, *Nature* **388**, 431 (1997).
5. G. Möller, M. Harke, H. Motschmann, *Langmuir* **14**, 4955 (1998).
6. S. Chandrasekhar, *Hydrodynamic and Hydromagnetic Stability* (Dover, New York, 1981).
7. M. van Dyke, *An Album of Fluid Motion* (Parabolic Press, Stanford, CA, 1982).
8. D. Quere, J.-M. di Meglio, F. Brochard-Wyart, *Science* **249**, 1256 (1990).
9. R. Bar-Ziv and E. Moses, *Phys. Rev. Lett.* **73**, 1392 (1994); R. Goldstein, P. Nelson, T. Powers, U. Seifert, *J. Phys. II Fr.* **6**, 767 (1996).
10. M. Struwe, *Plateau's Problem and the Calculus of Variations* (Princeton Univ. Press, Princeton, NJ, 1988).
11. J. Sullivan and F. Morgan, *Int. J. Math.* **7**, 833 (1996).
12. J. S. Rowlinson and B. Widom, *Molecular Theory of Capillarity* (Clarendon, Oxford, 1982).
13. P. Lenz and R. Lipowsky, *Phys. Rev. Lett.* **80**, 1920 (1998).
14. K. Brakke, *Exp. Math.* **1**, 141 (1990).
15. Some applications of the microchannel structures discussed here have already been patented (German Patent No. 197 48 295.3).

16. We acknowledge support by the Deutsche Forschungsgemeinschaft through the Schwerpunktprogramm 1052.

14 September 1998; accepted 20 November 1998

Sum Rules and Interlayer Conductivity of High-T_c Cuprates

D. N. Basov, S. I. Woods, A. S. Katz, E. J. Singley, R. C. Dynes, M. Xu,* D. G. Hinks, C. C. Homes, M. Strongin

Analysis of the interlayer infrared conductivity of cuprate high–transition temperature superconductors reveals an anomalously large energy scale extending up to midinfrared frequencies that can be attributed to formation of the superconducting condensate. This unusual effect is observed in a variety of materials, including $Tl_2Ba_2CuO_{6+x}$, $La_{2-x}Sr_xCuO_4$, and $YBa_2Cu_3O_{6.6}$, which show an incoherent interlayer response in the normal state. Midinfrared range condensation was examined in the context of sum rules that can be formulated for the complex conductivity. One possible interpretation of these experiments is in terms of a kinetic energy change associated with the superconducting transition.

Interlayer electron transport in cuprate superconductors has been the focus of both experimental and theoretical efforts (*1–11*). The radical differences between the in-plane and interlayer behaviors of cuprates are most clearly illustrated in the raw reflectance $R(\omega)$ measured with polarized light of frequency ω. In high transition temperature (T_c) superconductors, the reflectance of the electric field component parallel to the CuO_2 planes shows a metallic response, whereas reflectance obtained in the polarization along the interplane c axis direction [$R_c(\omega)$] is like that of ionic insulators with characteristic phonon peaks in the far infrared (IR), as shown in Fig. 1 for $Tl_2Ba_2CuO_{6+x}$ (Tl2201). Below T_c a sharp plasma edge at $\omega = 37$ cm^{-1} (in Tl2201) emerges out of a nearly "insulating" normal state spectrum because superconducting (SC) currents flow along all crystallographic directions. In other cuprate compounds, this feature appears at 10 to 200 cm^{-1} (*2–4, 12–15*). A collective (Josephson-like) mode associated with pair tunneling between CuO_2 layers implies a plasma edge in the IR reflectance with the frequency position of the minimum in $R_c(\omega)$ being proportional to the square root of the superfluid density ρ_s. The magnitude of ρ_s quantifies the electronic spectral weight of the SC δ function: $\rho_s = 4\pi n_s e^2/m^*$ (*16*), where n_s is the density of SC carriers, m^* is their mass, and e is the electron charge. Although development of the plasma edge is expected based on elementary electrodynamics (*6*), formation of the SC condensate from the incoherent normal state response is an intriguing issue.

We explored the changes in incoherent c-axis conductivity below T_c in connection with the c-axis superfluid density. Our analysis uses model-independent arguments based on the oscillator strength sum rule or causality of the electromagnetic response. We found that in several high-T_c cuprates, ρ_s significantly exceeds the spectral weight missing from the real part of the conductivity in a frequency region comparable to the SC gap 2Δ. This discrepancy in spectral weight indicates that a significant fraction of ρ_s is accumulated from mid-IR frequencies. These results support the hypothesis of a kinetic energy change associated with the superconducting transition (*5, 9, 17, 18*).

We measured the c-axis response of Tl2201 at the University of California at San Diego and compared our new data with earlier results reported by Timusk's group at McMaster University for lightly underdoped $La_{2-x}Sr_xCuO_4$ (La214) with $T_c = 32$ K (*12*) and underdoped $YBa_2Cu_3O_{6.6}$ (Y123) with $T_c = 59$ K (*13*). $Tl_2Ba_2CuO_{6+x}$ is a structurally simple material with just one CuO_2 plane per unit cell. Single crystals were grown as described in (*7*) and exhibited a SC transition at $T_c = 81$ K with $\Delta T_c \simeq 8$ to 10 K (from magnetization). Reflectance measurements in the frequency range from 16 to 15,000 cm^{-1} were performed with an IR interferometer upgraded for spectroscopy of microsamples. Typical dimensions of the Tl2201 crystals were $0.8 \times 0.8 \times 0.075$ mm^3. A mosaic of several specimens with similar T_c and ΔT_c was used for the measurements in the energy interval down to 16 cm^{-1}. The experiment was then repeated in the range from 60 to 9000 cm^{-1} using the thickest ($\simeq$130 μm) single crystal. The difference from the mosaic spectrum did not exceed 6%. The uncertainty of the relative changes in the spectra taken at different temperatures was less than 0.5%; this latter uncertainty

D. N. Basov, S. I. Woods, A. S. Katz, E. J. Singley, R. C. Dynes, Department of Physics, University of California–San Diego, La Jolla, CA 92093–0319, USA. M. Xu, James Franck Institute, University of Chicago, Chicago, IL 60637, USA. D. G. Hinks, Department of Materials Science, Argonne National Laboratory, Argonne, IL 60439, USA. C. C. Homes and M. Strongin, Department of Physics, Brookhaven National Laboratory, Upton, NY 11973–5000, USA.

*Present address: Lucent Technologies, 2000 North Naperville Road, Naperville, IL 60566, USA.

is of primary importance for analysis of the spectral weight detailed below.

The c-axis component of the complex conductivity of Tl2201 crystals $\sigma(\omega) = \sigma_1(\omega) + i\sigma_2(\omega)$ was determined through Kramers-Kronig (KK) transformations of the normal incidence $E \parallel c$ reflectance. Extrapolations to low and high frequencies required for KK integrals do not affect the results in the frequency range where the actual data exist. The real and imaginary parts of the conductivity (Fig. 2) are dominated by a series of phonon peaks (at 85, 153, 366, and 602 cm^{-1} in Tl2201). The electronic background is relatively weak and at $T \simeq T_c$ the dc conductivity inferred from $\sigma_1(\omega \rightarrow 0)$ is about 5 Ω^{-1} cm^{-1}. If we ignore phonon peaks and weak features in the electronic background of Tl2201 and La2l4, the conductivity can be described as $\sigma_1(\omega) \simeq \sigma_{dc}$ up to at least 200 meV (*19*). Featureless absorption with the spectral weight being almost uniformly spread over a broad energy scale is indicative of incoherent transport between the CuO_2 layers (*1*). Consistent with this view, $\sigma_2(\omega)$ is negative down to the lowest accessible energies, which suggests that the dominant contribution to the conductivity is due to IR-active phonons and possibly high-frequency electronic transitions.

Spectra of $\sigma_2(\omega)$ undergo a qualitative change with the SC transition: below T_c in all samples studied one finds a strong positive far-IR contribution. The SC δ function in $\sigma_1(\omega)$ implies (by causality of the electromagnetic response) a $1/\omega$ term in $\sigma_2(\omega)$ with a prefactor given by the superfluid density: $\sigma_2(\omega,T) = \rho_s(T)/4\pi\omega$. We determined the magnitude of ρ_s from extrapolation of $\omega\sigma_2(\omega)$ to zero frequency. This method of extracting ρ_s from the data does not require model-dependent assumptions. We used this value of ρ_s to calculate the spectra of $\sigma_2(\omega, T < T_c)$ from the following expression: $\sigma_2(\omega, T < T_c) = \rho_s(T)/4\pi\omega + \sigma_2(\omega, T > T_c)$ (Fig. 2 right, thin dashed lines). The spectra calculated in this fashion with no adjustable parameters reproduce the data in all the materials, thus validating the procedure of determining ρ_s.

The absolute values of the SC plasma frequency $\omega_{ps} = (\rho_s)^{1/2}$ for La2l4 and Y123 are in good agreement with the results reported by others (*2, 14*). Our value for Tl2201, $\omega_{ps} = 130$ cm^{-1}, is somewhat greater than the value of 98 cm^{-1} estimated from a fit of grazing incidence reflectance data to an oscillator model by Tsvetkov *et al.* (*20*). The magnitude of the c-axis penetration depth $\lambda_c = c/(\rho_s)^{1/2} \simeq 12$ μm from our data is shorter than $\lambda_c = 17$ to 19 μm measured by Moler *et al.* (*7*). We believe that the differences may be due to the sensitivity of the c-axis response of Tl2201 to minor variations of oxygen content or to structural defects acting as weak link interconnections between the CuO_2 planes. Clearly, these results call for systematic studies of the evolution of ρ_s with doping.

We now turn to analysis of the changes in the real, dissipative part of the conductivity $\sigma_1(\omega)$ below T_c. In all the crystals, the SC state conductivity is suppressed compared with the spectra taken at $T \simeq T_c$. None of the studied samples, however, reveal new features in $\sigma_1(\omega)$ at $T \ll T_c$ that can be assigned to the SC gap. Notably, $\sigma_1(\omega)$ remains finite down to the lowest frequencies, which suggests gapless behavior. We quantify the changes in the electronic background by introducing the effective spectral weight $N_{eff}(\omega)$:

$$N_{eff}(\omega) = \frac{120}{\pi}\int_{0+}^{\omega} d\omega'\sigma_1(\omega') \quad (1)$$

The magnitude of $N_{eff}(\omega)$ is proportional to the number of carriers participating in the optical absorption below the cutoff frequency ω and has the dimensions of the plasma frequency squared (cm^{-2}). It is instructive to compare Eq. 1 with the oscillator strength sum rule for optical conductivity that relates the integral of $\sigma_1(\omega)$ to carrier density n and free electron mass m_e:

$$\int_0^{\infty} d\omega\sigma_1(\omega) = \frac{\pi n e^2}{2m_e} \quad (2)$$

One difference between Eqs. 1 and 2 is that, in the latter, integration is performed up to ∞ and this model-independent sum rule insists that the area confined under the whole conductivity spectrum must be equal to a constant. On the contrary, N_{eff} defined according to Eq. 1 over an incomplete frequency range can be a temperature-dependent quantity. In both the La214 and Y123 materials, N_{eff} ($\omega < 700$ cm^{-1}) is

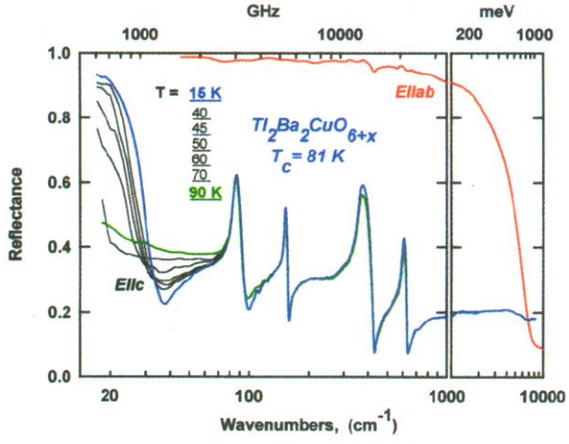

Fig. 1. Reflectance of $Tl_2Ba_2CuO_{6+x}$ measured in $E \parallel c$ and $E \parallel ab$ polarizations of incident radiation. The c-axis reflectance is nearly insulating in the normal state but at $T < T_c \simeq 80$ K is dominated by the Josephson-like plasma edge.

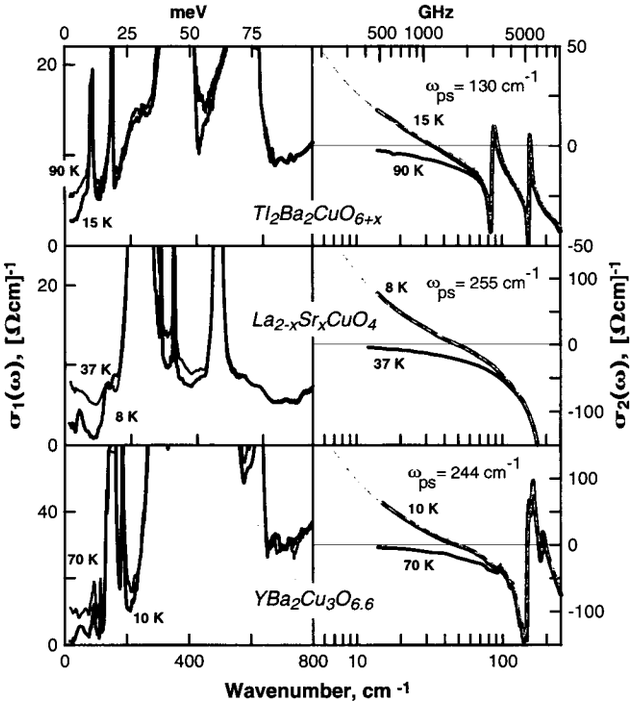

Fig. 2. **(Left)** The real part of the conductivity of $Tl_2Ba_2CuO_{6+x}$, $La_{2-x}Sr_xCuO_4$ (*12*) and $YBa_2Cu_3O_{6.6}$ (*13*). The sharp structure is due to IR-active phonons. **(Right)** The imaginary part of the conductivity at $T \simeq T_c$ and at $T \ll T_c$. Thin dashed lines show zero parameter fit to the superconducting state data calculated as described in the text. Data for $YBa_2Cu_3O_{6.6}$ are reprinted from *Physica C*, volume 254, C. C. Homes, T. Timusk, D. A. Bonn, R. Liang, W. N. Hardy, "Optical properties along the c-axis of $YBa_2Cu_3O_{6+x}$, for x = 0.50 to 0.95. Evolution of the pseudogap," pp. 265–280, Copyright, 1995, with permission from Elsevier Science.

strongly suppressed as T is lowered from 300 K down to T_c; this effect is usually attributed to a pseudogap leading to transfer of the electronic spectral weight from far-IR to higher energies (*3, 4, 14, 21*).

In conventional superconductors suppression of $\sigma_1(\omega)$ at $T \ll T_c$ is connected with the formation of SC condensate. Indeed, $\sigma_1(\omega) = 0$ for $T \ll T_c$ and ω below the energy gap 2Δ, with the "missing area" in the conductivity recovered under the δ function at $\omega = 0$ (Fig. 3 bottom). Then the conservation of the total spectral weight between the normal and SC state (N_n and N_s, respectively) is expressed in terms of the Ferrell-Glover-Tinkham sum rule (*22*):

$$\rho_s = N_n - N_s \qquad (3)$$

where $N_n = (120/\pi) \int_0^\infty d\omega\sigma_1(\omega, T > T_c)$ and $N_s = (120/\pi) \int_{0+}^\infty d\omega\sigma_1(\omega, T = 0)$. However, almost every property of the cuprates is anything but conventional. In particular, the absolute values of ρ_s and $[N_n(T \simeq T_c) - N_s]$ show no simple relation analogous to Eq. 3 between the ρ_s extracted from $\sigma_2(\omega)$ and the missing spectral weight determined from $\sigma_1(\omega)$ (Fig. 3) (*23*). It appears that the area confined under the SC δ function is nearly twice $[N_n(\omega) - N_s(\omega)]$ when the upper limit of integration in the latter is restricted to 120 to 150 meV.

We believe that the inequality $\rho_s > [N_n(T \simeq T_c) - N_s]$ originates from the limited frequency range over which the integration is performed. Nevertheless, the frequency scale in Fig. 3 is quite broad compared with the estimates of $2\Delta = 45$ meV based on photoemission studies (*24*) and is sufficient to exhaust the SC sum rule (Eq. 3) in a conventional dirty limit superconductor. In the dirty limit about 60% of ρ_s originates from $\omega < 2\Delta$, and by $\omega \simeq 6\Delta$ the accumulation of the condensate is 96% complete (Fig. 3 bottom). In cuprates we find that the spectra of $[N_n(\omega) - N_s(\omega)]/\rho_s$ show a very steep slope that saturates at $\omega \simeq 300$ cm^{-1} ($\simeq 38$ meV), reaching a value of approximately 0.5. The discrepancy between ρ_s and $(N_n - N_s)$ shows that the spectral weight of the c-axis condensate, at least in several different classes of cuprate superconductors, is collected from frequencies significantly exceeding 120 to 150 meV. The saturation of $[N_n(\omega) - N_s(\omega)]/\rho_s$ at $\omega \simeq 300$ cm^{-1} suggests that it is unlikely that the remaining portion of ρ_s will be acquired in the immediate vicinity of the upper-ω limit of our data. It is also unlikely that the high-energy contribution to the SC condensate is confined to some narrow feature located at $\omega > 150$ meV. Our accuracy in this region is sufficient to detect a sharp absorption resonance, which is not found in mid-IR energies. We therefore conclude that about 50% of the spectral weight of the condensate associated with the Josephson-like collective mode of cuprates is distributed over a broad frequency scale starting at 0.15 eV and extending through the mid-IR range (up to $\simeq 0.5$ eV or even higher energy). In the case of underdoped La214 and Y123 compounds, the presence of the pseudogap seen in the interplane conductivity implies that the mid-IR contribution to ρ_s is likely even stronger (*25*). It is interesting that the energy range from which the superconducting condensate is drawn and the energy scale for the pseudogap are comparable.

We emphasize that the $\rho_s > [N_n - N_s]$ inequality suggesting mid-IR condensation (Fig. 3) is specific only to the c-axis electrodynamics and only to the materials with truly incoherent normal state conductivity. So far, we have been unable to find similar conflict between the values of ρ_s and $[N_n - N_s]$ in the in-plane response of either Y123, La214, Tl2201, or any other cuprate. Also, the strength of the effect in the c-axis electrodynamics is suppressed as the c-axis response becomes more coherent with increasing doping. Specifically, for a series of YBCO crystals with different oxygen dopings, the discrepancy between ρ_s and $[N_n - N_s]$ is greatest in the $YBa_2Cu_3O_{6.53}$ compound and systematically decreases with increasing doping until the discrepancy vanishes for $YBa_2Cu_3O_{6.85}$. In addition, we have observed enhancement of ρ_s compared with the magnitude of $[N_n - N_s]$ in a series of Ni-doped $YBa_2Cu_3O_{6.6}$ crystals and in $YBa_2Cu_4O_8$ samples. Although there is no sign of the spectral weight discrepancy in optimally doped $YBa_2Cu_3O_{6.95}$ crystals with $T_c \simeq 93$ K, other cuprates with high values of T_c including Tl2201 and $HgBa_2CuO_4$ ($T_c \simeq 96$ K) (*26*) do exhibit the $\rho_s > [N_n - N_s]$ inequality. Considering the gapless nature of $\sigma_1(\omega)$ at $T \ll T_c$ in all these materials and the large energy scale of superfluid formation, one can conclude that the magnitude of the SC gap is irrelevant to the interlayer response at least of the cuprates discussed in this work. It remains to be seen whether evidence for mid-IR condensation is found in other cuprates or in other classes of strongly anisotropic noncuprate superconductors including 2D organic materials and $NbSe_2$.

The discrepancy between the magnitude of the superfluid density ρ_s and the spectral weight missing from the IR part of the conductivity can be interpreted within theoretical approaches that lead to the following form of the conductivity sum rule (*9, 10, 17, 27*)

$$\frac{120}{\pi}\left[\int_0^W d\omega\sigma_1(\omega, T)\right] = \alpha(T) \qquad (4)$$

In Eq. 4, W is a cutoff frequency of the order of a bandwidth and $\alpha(T)$ is proportional to an electronic kinetic energy (*5, 8–10, 17*). In these sum rules, the right-hand side of Eq. 4 is allowed to change with temperature, magnetic field, and other parameters. The validity of the global oscillator strength sum rule (Eq. 2) is assured through proper readjustment of high-energy interband contributions to $\sigma_1(\omega)$ at $\omega > W$. We stress that only the sum rule in Eq. 2 is truly model independent. For the case of a superconductor, Eq. 4 can be used to yield the following sum rule (*9, 10, 17*):

$$\rho_s = \frac{120}{\pi}\left[\int_{0+}^W d\omega(\sigma_1(\omega, T \simeq T_c) - \sigma_1^s(\omega, T \ll T_c))\right] + [\alpha_s - \alpha_n]$$
$$= [N_n - N_s] + [\alpha_s - \alpha_n] \qquad (5)$$

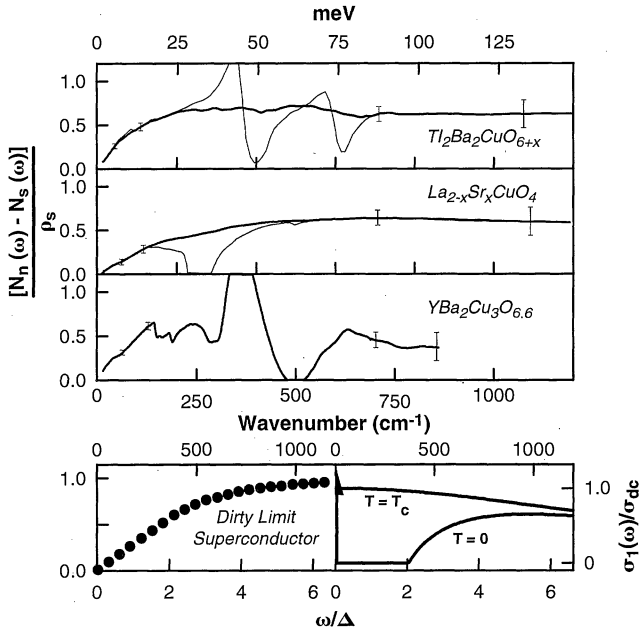

Fig. 3. (**Top**) Difference between the effective spectral weight at $T \simeq T_c$ and at $T \ll T_c$, normalized by ρ_s. In all the materials studied, $[N_n(\omega) - N_s(\omega)]/\rho_s$ did not exceed 0.6 (ignoring sharp peaks due to the IR-active phonons). In the case of $La_{2-x}Sr_2CuO_4$ and $Tl_2Ba_2CuO_{6+x}$ we show $[N_n(\omega) - N_s(\omega)]/\rho_s$ without phonon subtraction (light lines) and with phonons removed as described in (*12, 23*) (dark lines). Approximate error bars are shown at selected energies. (**Bottom left**) Calculations for a conventional dirty-limit superconductor with the scattering rate $\Gamma = 20\Delta$ show that about 90% of the ρ_s is collected from $\omega < 4\Delta$—that is, $[N_n(\omega) - N_s(\omega)]/\rho_s > 0.9$ by $\omega = 4\Delta$. This energy scale corresponds to about 0.1 eV in the case of the cuprates if the photoemission result for 2Δ is used (*24*). (**Bottom right**) Spectra of $\sigma_1(\omega)$ for a conventional dirty superconductor with $\Gamma = 20\Delta$.

where α_n and α_s are proportional to electronic (kinetic) energies in the normal and SC states. In our experiments, ρ_s and $[N_n - N_s]$ are obtained independently (*28*). Therefore, the inequality $\rho_s > [N_n - N_s]$ (Fig. 3) indicates that kinetic energy change associated with the SC transition may account for the discrepancy in spectral weight.

The change of the electronic kinetic energy at $T < T_c$ suggested by our data should be contrasted with the behavior of conventional superconductors where this effect is negligibly small. Moreover, in metallic superconductors $\rho_s - [N_n - N_s]$ ought to be negative, consistent with the experimental data for lead films (*29*). At least two models proposed for high-T_c superconductors (*17, 18*) predicted the correct sign of the effect but expected it to be dominant in the response of the CuO_2 planes. The interlayer tunneling (ILT) theory (*5, 8, 9*) predicted the $\rho_s > [N_n - N_s]$ inequality found in the *c*-axis transport, but the absolute value of ρ_s in Tl2201 is smaller (*7, 20*) than is expected within the ILT model (*5, 8*). Because change in the interlayer kinetic energy has been detected in several classes of high-T_c superconductors, we believe that this unusual effect will be instrumental in narrowing the field of plausible theoretical models of high-T_c superconductivity.

References and Notes

1. S. L. Cooper and K. E. Gray, in *Physical Properties of High-Temperature Superconductors IV*, D. M. Ginsberg, Ed. (World Scientific, Singapore, 1994), pp. 61–188.
2. K. Tamasaku, Y. Nakamura, S. Uchida, *Phys. Rev. Lett.* **69**, 1455 (1992); S. Uchida, K. Tamasaku, S. Tajima, *Phys. Rev. B* **53**, 14558 (1996).
3. C. C. Homes, T. Timusk, R. Liang, D. A. Bonn, W. N. Hardy, *Phys. Rev. Lett.* **71**, 1645 (1993).
4. D. N. Basov, T. Timusk, B. Dabrowski, J. D. Jorgensen, *Phys. Rev. B* **50**, 3511 (1994).
5. P. W. Anderson, *Science* **268**, 1154 (1995); P. W. Anderson, *The Theory of Superconductivity in the High-Tc Cuprates* (Princeton Univ. Press, Princeton, NJ, 1998); P. W. Anderson, *Phys. C* **11**, 185 (1991).
6. J. Schutzmann *et al.*, *Phys. Rev. B* **55**, 11118 (1997).
7. K. Moler, J. R. Kirtley, D. G. Hinks, T. W. Li, M. Xu, *Science* **279**, 1193 (1998).
8. P. W. Anderson, *ibid.*, p. 1196.
9. S. Chakravarty, *Eur. Phys. J.* **B5**, 337 (1998).
10. E. H. Kim, *Phys. Rev. B* **58**, 2452 (1998).
11. Y. Nakamura and S. Uchida, *ibid.* **47**, 8369 (1993); K. Takenaka, K. Mizuhashi, H. Takagi, S. Uchida, *ibid.* **50**, 6534 (1994); J. Schutzmann, S. Tajima, S. Miyamoto, S. Tanaka, *Phys. Rev. Lett.* **174**, 174 (1994); R. J. Radtke and K. Levin, *Phys. C* **250**, 282 (1995); A. A. Abrikosov, *Phys. Rev. B* **54**, 12003 (1996); A. J. Leggett, *Science* **274**, 587 (1996); S. E. Shafranjuk, M. Tachiki, T. Yamashita, *Phys. Rev. B* **55**, 8425 (1997); S. Das Sarma and E. H. Hwang, *Phys. Rev. Lett.* **80**, 4752 (1998); C. Bernhard *et al.*, *ibid.*, p. 1762.
12. D. N. Basov, H. A. Mook, B. Dabrowski, T. Timusk, *Phys. Rev. B* **52**, R13141 (1995).
13. C. C. Homes, T. Timusk, D. A. Bonn, R. Liang, W. N. Hardy, *Phys. C* **254**, 265 (1995).
14. S. Tajima *et al.*, *Phys. Rev. B* **55**, 6051 (1997).
15. H. Shibata and T. Yamada, *ibid.* **56**, 14275 (1997).
16. This definition of ρ_s implies that it has dimensions of the plasma frequency squared (cm^{-2}).
17. J. E. Hirsch, *Phys. C* **199**, 305 (1992); J. E. Hirsch, *ibid.* **201**, 347 (1992).
18. A. J. Leggett, *J. Phys. Chem. Solids*, in press.
19. In underdoped Y123 crystals one finds a step-like structure at 200 to 300 cm^{-1} (*3*). This step-like structure is not found in La214 or Tl2201 crystals.
20. A. Tsvetkov *et al.*, *Nature* **395**, 360 (1998).
21. V. J. Emery and S. A. Kivelson, unpublished.
22. M. Tinkham and R. A. Ferrell, *Phys. Rev. Lett.* **2**, 331 (1959).
23. In Fig. 3 the spectra of $[N_n(\omega) - N_s(\omega)]/\rho_s$ for Tl2201 and La214 are shown in two different forms. Thick lines show only the electronic contribution. In these spectra the contribution of phonons has been subtracted by fitting the phonon peaks in $\sigma_1(\omega)$ to Lorentzian oscillators. Thin lines show the data without phonon subtraction. In the case of Tl2201 and La214 crystals, phonon subtraction is well-justified because all the phonon peaks are narrow and show only weak asymmetry. In the case of $YBa_2Cu_3O_{6.6}$ a broad mode at 400 cm^{-1} appears that is very different from typical phonons in the conductivity spectra of crystalline solids (*3*). Therefore, the phonon contribution has not been removed. The narrowing and shift of the phonon modes produce strong oscillations in the spectrum of $[N_n(\omega) - N_s(\omega)]/\rho_s$ of all the crystals. The total oscillator strength of phonons is constant with temperature. Thus, the magnitude of $[N_n(\omega) - N_s(\omega)]/\rho_s$ in the high-frequency part of the spectrum characterizes the change in the electronic part of the conductivity relative to the strength of the SC δ function.
24. Z.-X. Shen *et al.*, *Science* **267**, 343 (1995); Ding *et al.*, *Nature* **382**, 51 (1996).
25. As mentioned above, in the La214 and Y123 materials N_{eff} at $T \simeq T_c$ is depressed compared with N_{eff} at $T = 300$ K, with spectral weight transferred from the far-IR to higher energies. Only in the case of the large La214 crystals was it possible to verify experimentally that Eq. 2 is obeyed and that the weight removed from the far-IR is recovered at $\omega > 0.5$ eV (*12*). In all other cases the minuscule size of single crystals precluded measurements in the mid-IR with the required accuracy. It appears that below T_c some of the high-energy spectral weight (*21*) is recovered under the superconducting δ function, whereas far-IR conductivity in the region related to the energy gap shows only a small depression below T_c. Because the reduction of the low-energy spectral weight at $T > T_c$ is well documented for both underdoped La214 and Y123 compounds (*3, 4, 14*), we believe that the suppression of $\sigma_1(\omega)$ at $T < T_c$ in these materials may be unrelated to superconductivity. Instead, the diminishing of $\sigma_1(\omega)$ below T_c can be attributed at least partially to the same process that leads to transfer of the spectral weight to higher energies in the pseudogap state at $T > T_c$. Alternatively, one would be forced to assume that development of the pseudogap is suddenly interrupted at $T = T_c$; this conflicts with studies of thermodynamic properties and of nuclear magnetic resonance, both of which display continuous behavior in the underdoped cuprates across T_c [J. W. Loram *et al.*, *Phys. Rev. Lett.* **71**, 1740 (1993); W. W. Warren Jr. *et al.*, *ibid.* **62**, 1193 (1989); R. E. Walstedt *et al.*, *Phys. Rev. B* **41**, 9574 (1990)]. Therefore, a 50% contribution of mid-IR frequencies to the spectral weight of the SC δ function should be regarded as a lower limit because arguments based on the continuity of the pseudogap development at T_c appear to indicate even stronger discrepancy between ρ_s and $[N_n - N_s]$, at least in the La214 and Y123 compounds. Our room temperature data for Tl2201 do not extend below 60 cm^{-1}, and the evolution of the electronic spectral weight at $T > T_c$ in this material requires further study.
26. E. J. Singley, D. N. Basov, G. Villard, A. Maignan, unpublished data.
27. P. F. Maldague, *Phys. Rev. B* **16**, 2437 (1977).
28. It was emphasized by Chakravarty that the normal state conductivity in Eqs. 3 and 5 has to be obtained at $T \rightarrow 0$ because some of the changes in $\sigma_1(\omega)$ at $T < T_c$ can be unrelated to superconductivity (*9*). This correct application of sum rules to the analysis of the IR data may further enhance the inequality between ρ_s and $[N_n - N_s]$.
29. L. H. Palmer and M. Tinkham, *Phys. Rev.* **165**, 588 (1968). The authors suggest that strong coupling effects account for most of the observed discrepancy between ρ_s and $[N_n - N_s]$.

30. We are grateful to J. E. Hirsch, S. Chakravarty, V. N. Muthukumar, T. Timusk, and V. J. Emery for valuable discussions. The work at the University of California at San Diego and Brookhaven was supported by the Department of Energy (DOE), Division of Materials Sciences, under contract DE-AC02-98CH10886; the Sloan Foundation; the Research Corporation; and AFOSR grant F4962-092-J0070. The work at Argonne was supported by National Science Foundation grant DMR 91-20000 and by DOE contract W-31-109-ENG-38.

17 August 1998; accepted 15 October 1998

Imaging Electron Wave Functions of Quantized Energy Levels in Carbon Nanotubes

Liesbeth C. Venema, Jeroen W. G. Wildöer, Jorg W. Janssen, Sander J. Tans, Hinne L. J. Temminck Tuinstra, Leo P. Kouwenhoven, Cees Dekker*

Carbon nanotubes provide a unique system for studying one-dimensional quantization phenomena. Scanning tunneling microscopy was used to observe the electronic wave functions that correspond to quantized energy levels in short metallic carbon nanotubes. Discrete electron waves were apparent from periodic oscillations in the differential conductance as a function of the position along the tube axis, with a period that differed from that of the atomic lattice. Wave functions could be observed for several electron states at adjacent discrete energies. The measured wavelengths are in good agreement with the calculated Fermi wavelength for armchair nanotubes.

Carbon nanotubes are molecular wires that exhibit fascinating electronic properties (*1*). Electrons in these cylindrical fullerenes are confined in the radial and circumferential directions and can only propagate in the direction of the tube axis. Nanotubes are therefore interesting systems for studying the quantum behavior of electrons in one dimen-